LOCALIZED DEFORMATION AND FRACTURE DUE TO LOW VELOCITY PARTICULATE EROSION OF DUCTILE METALS BY SPHERICAL PARTICULATES

P. S. Follansbee*, D. Banerjee and J. C. Williams****

**Formerly Department of Metallurgical Engineering and Materials Science Carnegie-Mellon University, Pittsburgh, PA. Now at Los Alamos National Laboratory, Los Alamos, NM 87544, USA*

***Department of Metallurgical Engineering and Materials Science Carnegie-Mellon University, Pittsburgh, PA 15213, USA*

ABSTRACT

A simple cumulative damage model has been developed for the low velocity, normal incidence erosion of ductile metals by spherical particles. The model correlates the computed plastic strain distribution for different impact velocities and materials with the experimentally measured erosion rates. This paper describes the surface and sub-surface changes which occur in Cu and Cu-6wt%Al specimens during erosion testing. Scanning and transmission electron microscopy have been used to study these changes. The object of this study was to determine whether the deformed microstructures are consistent with the predictions of the model. Because the deformation due to the impact of a 50μm diameter spherical particle occurs at high strain rates ($10^6 s^{-1}$) and is also highly localized, the deformation mechanisms differ slightly from bulk deformation which has been reported for low strain rates. The contribution of strain localization (adiabatic shear) and twinning will be discussed in light of the microstructural observations.

KEYWORDS

Low velocity erosion; cumulative damage model; surface and sub-surface damage structure; electron microscopy.

1. INTRODUCTION

Material wear by particle erosion has received increased attention recently due to the interest in the design and operation of coal conversion systems. In order to solve some of the problems associated with containment and transport of erosive streams, a number of research efforts have been initiated. Some of these investigations centered on the fluid dynamics of a particle laden gaseous or fluid stream, while others have focused on material wear mechanisms. The latter group has been divided roughly by the impact conditions being studied. Those interested in high impact velocities (> 50 m/s)

and oblique angles of impact have generally applied and extended Finnie's tool cutting or gouging models (Finnie, 1977). At lower impact velocities and at impact incidence angles closer to 90°, it no longer can be assumed that material removal occurs during each impact event; thus, some other erosion mechanism must be responsible for the observed wear.

Follansbee, Sinclair and Williams (1981) have analyzed the erosion process to see if, under the highly simplified conditions of low velocity (5 m/s to 50 m/s), normal incidence impact of rigid, spherical particles, the mechanism of erosive wear might be analogous to that responsible for metal fatigue. An erosion model was developed (Follansbee, 1981) which incorporated a fatigue failure criterion and which yielded predictions of relative erosion rate based only on results of a stress analysis of the indentation process and data determined from standard low cycle fatigue (LCF) tests. A comparison between predictions of the model and experimental erosion rate test results indicated good agreement for Cu and Cu-7.5wt%Al specimens eroded by 50μm diameter glass spheres travelling at impact velocities ranging from 7.5 m/s to 30.5 m/s.

In this paper, we describe in more detail the surface and sub-surface observations obtained from such erosion specimens using scanning electron microscopy (SEM) and transmission electron microscopy (TEM). We will show that the observed microstructures are consistent with the cumulative damage or fatigue fracture model which has been proposed. We also will discuss the effect of strain rate on the microstructure and rate controlling erosion mechanism.

2. EXPERIMENTAL PROCEDURE

The present investigation combines the results of finite element stress analysis of the indentation event, measurement of weight loss in an erosion test, and microscopic characterization of surface and sub-surface features present in test specimens after erosion. Copper was chosen for study because it is a simple, single phase, well characterized, ductile FCC metal suitable for a modelling study. In addition, experiments were conducted using Cu-7.5Al because this material exhibits planar slip due to its low stacking fault energy. The difference in slip character, which is related to stacking fault energy, leads to distinct differences in both monotonic and cyclic deformation behavior, especially low cycle fatigue (Laird, 1967). The choice of a system with well documented low cycle fatigue behavior was a primary consideration for these experiments. The impacting material was glass spheres with an average diameter of 50μm.

Details of the stress analysis techniques used to predict erosion rates and the erosion test apparatus used to perform erosion experiments are given by Follansbee (1981).

The morphologies of eroded surfaces, sub-surface regions, and wear debris were characterized with SEM. The erosion test specimens are small enough to fit intact into the specimen chamber of the JOEL JSM35 microscope used for the surface studies. This allowed examination of the entire eroded surface at various stages of weight loss. Sub-surface regions were prepared for SEM according to the following procedure. A layer of Cu was first electrodeposited on the eroded surface in an aqueous solution of 250 gm/liter $CuSO_4 \cdot H_2O$ and 75 gm/liter H_2SO_4 (Ives, 1977). Slices normal to the eroded surface were cut with a slow speed diamond saw. These surfaces only required light polishing with Linde A and Linde B. Care was taken to not over-polish which could disrupt the regions just below the eroded surface. Although polished surfaces

exhibit poor definition in the microscope, some of the slices were examined in this condition. Others were polished electrolytically in equal parts of nitric acid and methanol at room temperature to enhance surface definition.

Samples for TEM studies of erosion damage were made from annealed Cu (cold worked 30% and annealed at 600°C for one hour) and annealed Cu-6.5%Al. Strips of these materials, 1mm thick, were eroded for two hours by glass beads striking at normal incidence with a velocity of 24.7 m/sec. After erosion the samples were flash plated with nickel from a Watts bath and then with OFHC copper using the Cu plating technique mentioned earlier, until a total thickness of 4mm was reached. Cross-section slices 0.4mm thick were removed from these samples so that the eroded surface was perpendicular to the plane of the section. These slices were then mechanically thinned down to 0.2mm, and 3mm diameter discs were punched from these slices keeping the interface between the electroplated deposit and the eroded surface at the center of the disc. These discs were electropolished in a Fischione Jet Polisher in a solution of 33% nitric acid in methanol. It often was difficult to obtain thin areas exactly at the interface, and ion-milling was used to extend the thin portions to the interface.

3. RESULTS

We include in this section a brief summary of results obtained by Follansbee, Sinclair and Williams (Follansbee, 1981) to provide a background for the microstructural observations. These include a description of the modelling of the erosion process and prediction of the erosion rates. We then describe in some detail the microstructural observations on the eroded samples.

3.1 Stress Analysis and Erosion Modelling

Following Mamoun (1975a&b), Follansbee (1981) assumed that the erosion rate was proportional to the cycles to failure (N_f) in a fatigue test, multiplied by the volume of material undergoing strain reversals. Thus, they obtain

$$\frac{\dot{E}_1}{\dot{E}_2} = \frac{A_2}{A_1} \frac{\varepsilon_2^{n_2}}{\varepsilon_1^{n_1}} \frac{V_1}{V_2} \qquad (1)$$

using the Coffin Manson law

$$N_f = A\varepsilon^n \qquad (2)$$

where $\dot{E}$ and $\dot{E}_2$ are the rates of erosion of two materials, and V is the volume experiencing the strain ε. A and n are constants for a given material.

ε and V are obtained from a finite element analysis as a single impact event by a rigid, spherical indenter (Follansbee, 1981). A typical result of the finite element analysis is shown in Figure 1. The maximum plastic strain is seen to occur in the near surface region at the edge of the contact area, and the strain-state in this location is one of pure shear. The stress analysis indicates that no significant strain reversal occurs on unloading the sphere. However, a significant strain reversal can occur if a second particle impacts at a point which is located at a 'mirror image' position with respect to the point of pure shear of the first particle.

A set of data obtained from the erosion rate experiments described earlier (Follansbee,1981) is shown in Figure 2. A steady-state weight loss is seen to follow a transient period.

The steady-state erosion rates derived from these curves (obtained at various impact velocities) were compared with predicted erosion rates, as shown in Table 1.

TABLE 5 Predicted and Measured Relative Erosion Rates

	Cu 15m/sec	Cu 30m/sec	Cu-Al 25m/sec
Predicted $\dot{E}/\dot{E}_o$	0.18	2.01	0.45
Measured $\dot{E}/\dot{E}_o$	0.17	1.90	0.39

The measured erosion rates are normalized by the measured value of Cu at 25m/sec ($\dot{E}_o$), and the predicted rates are also relative to that predicted for Cu at 25m/sec (also denoted $\dot{E}_o$).

3.2 Microstructural Characterization of Erosive Wear

Included in Figure 2 are SEM micrographs of typical surface regions at various stages of weight loss. The eroded surfaces are characterized by platelet formation from the very early stages of exposure (10^8 impacts). As the time of corrosion increases, a large density of voids appear on the surface. Figure 3(a) shows detail of a platelet held to the surface by only a small ligament.

Although 10^8 impacts corresponds to the first measurable weight loss in Figure 2, this stage of erosion is actually a relatively advanced stage when expressed in terms of degree of deformation of the specimen surface. To see this, note that 10^8 impacts over the entire surface corresponds to approximately 10^3 impacts over an area the size of a single impact crater (Follansbee, 1981). In addition, the estimated weight of a single wear particle (see Fig. 7 in Follansbee, 1981) is 4×10^{-10} grams which is six orders of magnitude below the resolution of the analytical balance used in this investigation. The observation of well-developed platelets after only 10^8 impacts further verifies that deformation is extensive at this early stage. These early stages of weight loss are convenient to study in that, as argued, sub-surface deformation should be well-developed, whereas a high density of voids, which complicate TEM of sub-surface regions, are not present. Thus, for the remainder of this paper, we will concentrate on observations at these early exposure times.

Sub-surface regions of specimens exposed to 10^8 impacts have been prepared for SEM according to the procedure outlined previously. At low and high magnifications the sub-surface regions are relatively featureless. Voids and embedded glass fragments are rarely found. Sub-surface crack patterns, as shown in Figure 3(b), are occasionally observed. The thumbnail pattern seen in these figures is the typical configuration of these crack patterns, although in some cases only half of the thumbnail crack is observed.

A detailed observation of the dislocation substructure resulting from erosion was carried out for the annealed Cu sample. A high density of dislocation dipoles were observed in a zone area extending from 60 to 100μm beneath the eroded surface (Fig. 4(a)). Beyond this depth deformation substructure was practi-

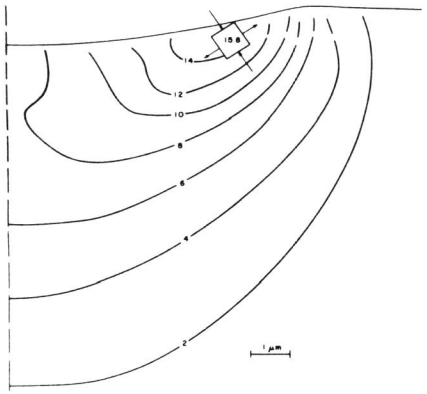

Fig. 1. Computed octahedral strain contours for maximum penetration for impact on copper at 24.7 m/sec.

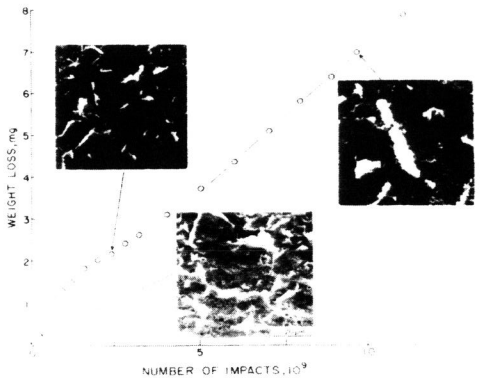

Fig. 2. The weight loss behavior of annealed copper eroded at 24.7 m/sec. Scanning electron micrographs are superimposed on the weight loss curve to illustrate the evolution of surface morphology.

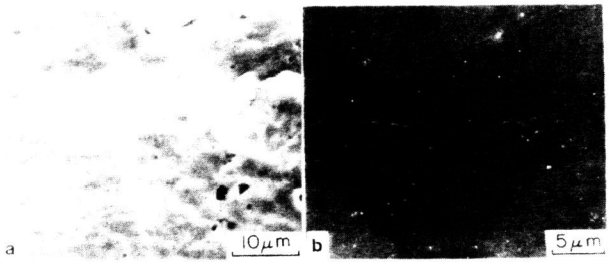

Fig. 3. a)Detail of platelet separation from the surface of copper at the early stages of erosion (10^8 impacts at 24.7 m/sec). b) In the same condition microstructure of sub-surface shows details of crack formation.

cally absent. The beginning of cell wall formations were seen at a depth of about 40μm beneath the surface. The zone 30-40μm from the surface consisted of diffuse equiaxed cell walls with a low dislocation density within the cells (Fig. 4(b)). The cell walls sharpened considerably in regions closer to the surface (10-30μm) and cells were, in general, elongated with a width of 0.4-0.5μm. Figure 4(c) shows an area just beneath the eroded surface (0-2μm). Here, well-defined equiaxed grains with a size of 0.2-0.3μm are seen with a high random dislocation density within them. The associated selected area diffraction (Fig. 4(d)) shows fairly sharp spots clustered in certain zones. The combination of the SAD and the image suggests that dynamic recrystallization has occurred just below the eroded surface. The substructure in all regions is very uniform and no indication of adiabatic shear or twinning were recorded.

The substructure in the Cu-6.5%Al alloy is quite different. The regions just below the eroded surface (0-3μm) consist of fine slip bands and a heavy dislocation density (Fig. 5(a)). The dislocation density decreases appreciably within 5μm of the eroded surface to isolated partials and non-extended dislocations (Fig. 5(b)).

4. DISCUSSION

The microstructures observed by TEM are qualitatively consistent with the nature of deformation predicted by the finite element analysis of the impact event. At distances 5-10μm below the eroded surface, the analysis predicts strains ranging from 1 to 5%. The cell structures observed 10-30μm below the eroded surface of annealed Cu bear a strong resemblance in size (0.4-0.5μm) as well as in the cell wall appearance to the substructures documented by others (Feltner, 1967) for cyclic loading at these strain levels. At distances greater than 40μm below the surface, no cell structure is observed but a high uniform density of dislocation dipoles and small dislocation loops exists. This structure also is characteristic of cyclic (rather than uniaxial) deformation at very low strain ranges (less than 0.05%) (Segall, 1959).

At portions just below the eroded surface (0-2μm) sharp, fine equiaxed grains are observed with a high dislocation density within them. The SAD from these areas shows sharp spots clustered around certain zones. Dynamic recrystallization cannot be ruled out in this region. However, no evidence of shear band formation or twinning, as observed by Kosel (1979) and others (Winter, 1975) was seen in this study. The deformation substructures were quite uniform. These observations are generally identical to those reported by Ives (1977). In the latter experiments, however, the eroding particles were angular Al_2O_3 which severely intensified deformation in the immediate sub-surface regions.

No cell structure was observed in the Cu-6.5%Al alloy. The dislocations were arranged in planar arrays and a high density of slip bands was observed. This is consistent with the low stacking fault energy of this material (Feltner, 1967; Saxena, 1975). The dislocation density dropped off very rapidly with increasing depth below the eroded surface which probably reflects the more rapid work hardening of Cu-Al compared to pure Cu. Here, also, the deformation patterns agree quite well with the deformation levels predicted by the finite element analysis.

The absence of deformation twinning, or severe strain localization, in the subsurface regions raises the question of strain rate effects. The lack of evidence in the microstructure of deformation features which normally correspond to the high strain rates that were estimated is surprising. Perhaps, however,

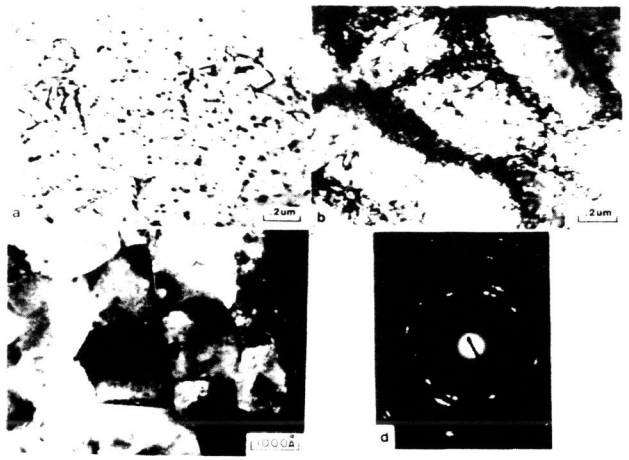

Fig. 4. Transmission electron microscopy of the substructure in annealed copper in the early stages of erosion (10^8 impacts at 24.7 m/sec). a)Dipoles and loops observed 60-100 microns below the eroded surface. b)Diffuse cell walls 30-40 microns below the eroded surface. c)Strongly misoriented equiaxed grains exist up to 5 microns below the eroded surface. The surface is shown in dotted lines on the micrograph. d)SAD from the area in (c).

Fig. 5. Transmission electron microscopy of eroded substructure in Cu-6Al in the early stages of erosion (10^8 impacts at 24.7 m/sec). a)Slip bands formed 2-5 microns below the eroded surface. b)Stacking faults and randomly oriented dislocations 5-10 microns below the eroded surface.

this emphasizes that strain rate effects are not well understood. In particular, it may not be correct to assume that the response to highly localized deformation (with respect to a structure parameter such as the grain size) should be the same as that documented for large-scale deformation. Our results suggest that the role of scale of deformation relative to microstructural scale may be more important than has been generally acknowledged.

4.1 Possible Void Formation Mechanism

The high density of dislocation loops and dipoles observed with TEM is also consistent with cyclic loading. The creation of vacancies at jogs in moving screw dislocations is conceptually well-known (Read, 1953; Mott, 1951), and Cottrell has suggested that the generation rate is enhanced by cyclic loading (Cottrell, 1957). Segall and Partridge (1959) reported a high density of dislocation loops in Al deformed by fatigue. The formation of pores, ostensibly from the condensation of vacancies, is also well documented. Rosi and Abrahams documented pore formation in Cu under low strain rate uniaxial strain (Rosi, 1960). That pore formation is a thermally activated process was demonstrated by Koppenaal who observed pores in single crystals of Cu-10Al deformed at low strain rate at room temperature but none in identical specimens deformed at 77 K (Koppenaal, 1961).

There is a direct correlation between these observations and evidence from erosion test specimens. It might be speculated that at least in the case of Cu, the sub-surface regions experience cyclic loading which leads to vacancy generation through dislocation intersections, as evidenced by the high density of dislocation loops. The coalescence of these vacancies into voids, however, is a thermally activated process and requires time or temperature. The time dependence of void growth in these erosion experiments is verified by the series of micrographs in Figure 2. The situation is less clear for Cu-Al since many fewer dislocation loops are observed. The formation of loops by dislocation interaction is less common in low stacking fault energy materials. Vacancies can still be created by non-conservative motion of jogs, however,

4.2 Platelet Formation

All of the microscopic evidence obtained from the Cu and Cu-6Al erosion specimens examined in this investigation emphasize the importance of the formation and subsequent fracture of platelets as the operative material removal mechanism. Platelets partially separated from the surface were a dominant feature of the surface morphology. The size and shape of the wear debris particles match closely the appearance of platelets seen on the surface. Further, the number or density of platelets found on the surfaces as a function of impact velocity follows the measured variation in erosion rate. Thus, we conclude that material removal is directly related to the formation of platelets on the eroded surface. We also note that platelet formation during erosion has already been extensively documented (Bellman,1980; Brown,1981; Rickerby,1979).

The results of the stress analysis of an indentation are consistent with the observation of platelet formation. The maximum plastic strains were shown to develop near the edge of the contact area. As described previously (Follansbee, 1981), the stress state at this location of maximum plastic strain is close to pure shear, and the plane of maximum shear strain is seen to be almost parallel to the surface. The magnitude of the plastic strains decreases rapidly with depth below the surface, but less rapidly along the surface toward the point of initial contact. All of these results agree with the shape, location, and dimension (thickness) of the observed platelets.

It would be difficult to predict the nucleation and growth of a crack beneath the particle impact zone in these complex and non-uniform loading conditions. Such predictions are currently only feasible for simple geometries in well characterized materials tests. But it might be speculated that after sufficient plastic strain reversals, cracks nucleate on the surface at the edge of the most recent indentation. Initial crack growth would be along the plane of maximum shear which is not quite parallel to the surface. As the crack enters the region of decreasing plastic strain amplitude, the path turns parallel to the surface and either connects with another crack or leads to separation of the cracked platelet from the substrate.

The evidence described here supports the cumulative damage model for low velocity particulate erosion. This evidence includes 1) the good agreement between measured and predicted erosion rates, the latter resulting from a simple model based only on an elasto-plastic stress analysis and on data from standard low cycle fatigue tests, and 2) the correlation between microstructures in fatigue test specimens and erosion test specimens described here. Vacancy generation and subsequent void formation is also consistent with cyclic deformation. Finally, the events leading to platelet formation have been described from results of the stress analysis and sub-surface microscopic observations.

Finally, we comment that the weight loss transient seen during the early stages of erosion (cr Fig. 2) may be related to the in-situ grain size refinement which occurs at the surface of the specimen. From our TEM observations, it can be seen that a very fine (< 1μm) recrystallized grain size develops during the initial stages of erosion exposure. Once developed, this fine-grained zone should have a greater fatigue resistance than the coarser-grained starting structure (Laird, 1967). Accordingly, we suggest that the initial higher weight loss rate is characteristic of the starting structure, whereas the lower, steady-state weight loss rate is characteristic of the fine-grained steady-state structure. We must also point out that the formation of a steady array of voids may also contribute to the transient in the weight loss curves. At this juncture our results do not permit the relative contributions of these two factors to be estimated. From our standpoint, it seems more important at present to suggest that the weight loss transient reflects an in-situ structural change which occurs during the erosion experiment. It is such changes that may complicate comparison of erosion data obtained under different experimental conditions.

It is important to emphasize once again the limited conditions over which these observations and conclusions apply. The simplified conditions of normal incidence impact of rigid, spherical particles at low impact velocities were purposely chosen to investigate the cumulative damage erosion model. Even in these conditions the time dependent formation of voids and eventual presence of fragmented and embedded glass complicate such a model. At early stages of erosion before these complications apply, however, the observations support the importance of cumulative damage in erosive wear.

ACKNOWLEDGMENTS

The authors gratefully acknowledge useful discussions with Prof. G. B. Sinclair and the experimental assistance of Messrs. C. Vallance and M. Glatz. This work has been supported by the Basic Energy Sciences Division of the Department of energy.

REFERENCES

Bellman, R., Jr. and Levy, A. (1980). Erosion mechanism in ductile metals. Technical Report, Lawrence Berkeley Laboratory, LBL-10289 Reprint.

Brown, R., Jun, E.-J. and Edington, J. W. (1981). Mechanisms of erosive wear for 90° impact on copper and iron targets. Wear, vol. 74, pp. 143-156.

Cottrell, A. H. (1957). Point defects and the mechanical properties of metals and alloys at low temperatures. Vacancies and Other Point Defects in Metals and Alloys, Institute of Metals, London, pp. 1-39.

Feltner, C.E. and Laird, C. (1967). Cyclic stress-strain response of f.c.c. metals and alloys-II. Acta Met., vol. 15, pp. 1638-1653.

Finnie, I., Levy, A. and McFadden, D. H. (1977). Fundamental mechanisms of the erosive wear of ductile metals by solid particles. W. F. Adler (Ed.), Erosion: Prevention and Useful Applications, American Society for Testing and Materials, ASTM STP 664, pp. 36-58.

Follansbee, P. S., Sinclair, G. B. and Williams, J. C. (1981). Modelling of low velocity particulate erosion in ductile metals by spherical particles. Wear, vol. 74, pp. 107-122.

Ives, L. K. and Ruff, A. W. (1977). Electron microscopy study of erosion damage in copper. W. F. Adler (Ed.), Erosion: Prevention and Useful Applications, American Society for Testing and Materials, ASTM STP 664, pp. 5-35.

Koppenaal, T. J. (1961). Porosity in plastically deformed Cu-10at%Al single crystals. Acta Met., vol. 9, pp. 1078-1079.

Kosel, T. H., Scattergood, R. O. and Turner, A.P.L. (1979). An electron microscopy study of erosive wear. Wear of Materials, American Society of Mechanical Engineers, pp. 192-204.

Laird, C. and Feltner, C. E. (1967). The Coffin-Manson law in relation to slip character. TMS-AIME, vol. 239, pp. 1074-1083.

Mamoun, M. M. (1975a). Materials Science Division Coal Technology Second Quarterly Report. Technical Report ANL-75-XX-2, Argonne National Laboratory, Appendix 1: Analytical models for the erosive-corrosive wear process.

Mamoun, M. M. (1975b). Materials Science Division Coal Technology Third Quarterly Report. Technical Report ANL-75-XX-3, Argonne National Laboratory, Appenxix 1: Analytical models for the erosive-corrosive wear process.

Mott, N. F. (1951). The mechanical properties of metals. Proceedings Physical Society, London, vol. B64, pp. 729-741.

Read, W. T. (1953). Dislocations in Crystals. McGraw-Hill, New York, p. 85.

Rickerby, D. G. and MacMillan, N. H. (1979). Mechanisms of solid particle erosion in crystalline materials. Proceedings of the 5th International Conference on Erosion by Solid and Liquid Impact, Cambridge, England, pp. 120-130.

Rosi, F. D. and Abrahams, M. S. (1960). Porosity in plastically deformed single crystals. Acta Met., vol. 8, p. 807.

Saxena, A. and Antolovich, S. D. (1975). Low Cycle fatigue, fatigue crack propagation and substructures in a series of polycrystalline Cu-Al alloys. Metall. Trans., 6A, pp. 1809-1828.

Segall, R. L. and Partridge, P. G. (1959). Dislocation arrangements in aluminum deformed tension of by fatigue. Philosophical Magazine, Series 8, vol.4, pp. 912-919.

Winter, R. E. and Hutchings, I. M. (1975). The role of adiabatic shear in solid particle erosion. Wear, vol. 34, pp. 141-148.